Received: 26 February 2022 | Revised: 28 March 2022 | Accepted: 8 April 2022

DOI: 10.1002/aoc.6696

RESEARCH ARTICLE

Applied Organometallic Chemistry WILEY

Quinoline-fused both non-peripheral and peripheral Zn^{II} and Mg^{II} phthalocyanines: Anti-cholinesterase, anti-α-glucosidase, DNA nuclease, antioxidant activities, and in silico studies

Halise Yalazan[1] | **Burak Tüzün**[2] | **Didem Akkaya**[3] | **Burak Barut**[3] | **Halit Kantekin**[1] | **Sermet Yıldırmış**[3]

[1]Faculty of Sciences, Department of Chemistry, Karadeniz Technical University, Trabzon, Turkey

[2]Plant and Animal Production Department, Technical Sciences Vocational School of Sivas, Sivas Cumhuriyet University, Sivas, Turkey

[3]Faculty of Pharmacy, Department of Biochemistry, Karadeniz Technical University, Trabzon, Turkey

Correspondence
Dr. Halit Kantekin, Department of Chemistry, Karadeniz Technical University, 61080 Trabzon, Turkey.
Email: halit@ktu.edu.tr

Quinoline-fused Zn^{II} (**$ZnPc^{p}$/$ZnPc^{np}$**) and Mg^{II} (**$MgPc^{p}$/$MgPc^{np}$**) phthalocyanines with four 4-methylquinolin-2-ol (**1**) at non-peripheral or peripheral positions of the phthalocyanine core have been synthesized via cyclotetramerization of phthalonitrile derivatives (**CN^{p}/CN^{np}**) in the presence of zinc (II) and magnesium (II) metal ions in this study. After synthesis and characterization processes, anti-cholinesterase, anti-α-glucosidase, DNA nuclease, antioxidant activities, and in silico calculations of both peripheral and non-peripheral Zn^{II} and Mg^{II} phthalocyanines were investigated. The inhibitory effects of metallated phthalocyanines on acetylcholinesterase, butyrylcholinesterase, and α-glucosidase enzymes were tested by spectrophotometric method. Theoretical methods are used to compare both the chemical and biological activities of the studied phthalonitrile derivatives and metallated phthalocyanine compounds.

KEYWORDS

anti-cholinesterase, anti-α-glucosidase, molecular docking, phthalocyanine, PLIP-

1 | INTRODUCTION

Alzheimer's disease (AD), a neurodegenerative disease, is usually seen in elderly people and causes amnesia and decreased cognitive functions in daily life.[1,2] Many factors are involved in the formation of AD disease such as reactive oxygen species, people's lifestyle, diabetes, environmental factors, cardiovascular diseases, acetylcholine deficiency, hypertension, and overproduction of β-amyloid peptide. Today, the exact cause of this disease, which is very important for people, has not been determined exactly, and a permanent solution has not been found.[3–6] The manufactured drugs only reduce the symptoms of this disease and slow down the worsening of the patient's condition. In recent years, researchers have focused on cholinesterase inhibitors. Although cholinesterases increase cholinergic nerve conduction by inhibiting cholinesterases, they reduce the level of acetylcholine in the brain and catalyze the hydrolysis of the neurotransmitter acetylcholine.[7,8]

Diabetes mellitus (DM) is a complex disease that causes serious complications with its high blood sugar level in the human body and is caused by the body's resistance to insulin or its deficiency.[9–11] The exact cause of DM disease has not yet been determined; however, when studies are examined, it has been seen that the main causes of this disease are genetic factors, environmental, and lifestyle.[12] α-Glucosidase, which plays a very important role in the treatment of DM, is located in the epithelial wall of the small intestine and its inhibitors reduce the

level of glucose in the bloodstream and is an important enzyme that plays a role in the digestion of carbohydrates.[13,14]

Theoretical calculations have become very common nowadays. In recent studies, molecular activities are reinforced by comparing theoretical calculations with experimental results.[15,16] The results obtained will guide many future studies. It is possible to compare the activities of molecules with quantum chemical calculations of molecules.

Phthalocyanines (Pcs) are aromatic macrocyclic compounds used in various applications due to their different binding positions, various coordination properties, and good spectroscopic characteristics.[17,18] Phthalocyanine compounds are used in many contemporary application areas such as photoluminescence,[19] photocatalytic,[20] photothermal activity,[21] non-linear optical (NLO),[22] and photodynamic therapy.[23] The aggregation and low solubility of these compounds in known organic solvents restrict their use in many modern biological applications. This situation disappears with the binding of appropriate substituents at peripheral and non-peripheral positions. It has been reported in studies that researchers examined that phthalocyanine derivatives containing substituted groups such as aryloxy, alkoxy, alkyl, alkylthio chains, and bulky groups have better solubility.[24]

Substituents attached to the phthalocyanine core are the most important factors affecting their use in many modern application areas. In this study, we wanted to examine the biological activity properties of quinoline-fused phthalocyanine compounds. Quinolines, which are among the nitrogen heterocyclic compounds, are versatile compounds with very important therapeutic potential.[25] The synthetic versatility of these compounds facilitates their use in a wide variety of biological activities.[26–28] There are many studies in the literature on acetylcholinesterase (AChE), butyrylcholinesterase (BuChE), and glucosidase enzymes of cobalt and copper phthalocyanines.[29–36] Besides, there are very few studies on these properties of phthalocyanine compounds containing quinoline groups. In this study, we wanted to examine these properties of quinoline substituted zinc and magnesium phthalocyanines, unlike the literature.

The study presents Zn^{II} (**$ZnPc^{p}$/$ZnPc^{np}$**) and Mg^{II} (**$MgPc^{p}$/$MgPc^{np}$**) phthalocyanines each fused with quinoline at peripheral or non-peripheral locations. In the literature, there are studies on the use of quinoline substituted phthalocyanine compounds in many different application areas.[37–41] The aim of this study is to demonstrate the effectiveness of new phthalocyanine compounds fused with quinoline against Alzheimer's (AD) and DM diseases with experimental approaches. Besides, we have presented computationally the biological activities of all compounds against different cancer proteins. The inhibitory effects of the quinoline-fused phthalocyanines on acetylcholinesterase (AChE), butyrylcholinesterase (BuChE), and glucosidase enzymes were tested by spectrophotometric method. In addition, the nuclease activity studies of these compounds on the supercoiled plasmid pBR322 DNA were investigated using the agarose gel electrophoresis method. Chemical calculations of all compounds were made in B3LYP,[42,43] HF,[44,45] and M062x[46] methods with 6- to 31-g basis set using Gaussian software. However, the biological activities of the all compounds with cancer proteins were compared. If these proteins are the crystal structure of estrogen receptor protein (from the breast cancer), ID: 1A52,[47] crystal structure of VEGFR kinase protein (from liver cancer), ID: 3WZE,[48] crystal structure of MLK4 kinase (colon cancer) ID: 4UYA,[49] and crystal structure of an allosteric Eya2 phosphatase inhibitor protein (from lung cancer), ID: 5ZMA.[50] Afterwards, Protein-Ligand Interaction Profiler (PLIP) analysis[51] was performed to examine the interactions between all compounds and proteins. The types of interactions that occurred were determined.

2 | EXPERIMENTAL

The used materials, equipment, acetylcholinesterase (AChE), butyrylcholinesterase (BuChE), α-glucosidase inhibitory, DNA hydrolytic nuclease, DPPH radical scavenging, and theoretical methods are presented as supporting information.

2.1 | Syntheses

2.1.1 | Quinoline-fused phthalonitrile derivatives (**CN^{p}/CN^{np}**)

4-methylquinolin-2-ol (**1**) (1.00 g, 6.28 mmol) was solved in dry DMF; after dissolution, 4-nitrophthalonitrile (**2a**) or 3-nitrophthalonitrile (**2b**) (1.09 g, 6.28 mmol) was added into the reaction content. Then, anhydrous potassium carbonate (2.60 g, 18.80 mmol) was added and the reaction mixture was continued with stirring at 56°C under N_2 atm, for 138 h. The crude product, poured onto ice and filtered, was crystallized from ethanol. Consequently, title compounds (**CN^{p}/CN^{np}**) were obtained as fawn colored solid products. The data of the **CN^{p}/CN^{np}** were given below.

*4-(4-methylquinolin-2-yloxy)phthalonitrile (**CN^{p}**)*
Yield: 64% (1.14 g).
Melting point: 185–188°C.
Solubility: Chloroform, ethyl acetate, dichloromethane.

FT–IR (ATR), υ_{max} (cm^{-1}): 3072–3,041 (Ar–H), 2889–2817 (Aliph. C–H), 2234 (C≡N), 1655, 1585, 1488, 1332, 1247–1210–1178 (Ar–O–Ar), 1095, 987, 839, 756.

^{1}H NMR ($CDCl_3$), (δ:ppm): 7.98–7.96 (d, H, $J = 8$ Hz, Ar–H), 7.79–7.70 (m, 3H, Ar–H), 7.52 (s, H, Ar–H), 7.42 (s, H, Ar–H), 7.13 (s, H, Ar–H), 6.59 (s, H, Ar–H), 2.52 (s, 3H, $-CH_3$).

^{13}C NMR ($CDCl_3$), (δ:ppm): 164.09, 159.65, 135.24, 133.92, 130.54, 130.08, 129.30, 128.31, 127.79, 125.60, 124.51, 123.88, 122.54, 120.58, 116.87 (C≡N), 116.45 (C≡N), 112.47, 19.21.

MALDI–TOF–MS *m*/z: Calculated for $C_{18}H_{11}N_3O$: 285.30; Found: 285.35 $[M]^+$.

*3-(4-methylquinolin-2-yloxy)phthalonitrile (**CN^{np}**)*
Yield: 55% (0.98 g).
Melting point: 189–193°C.
Solubility: Chloroform, ethyl acetate, dichloromethane.

FT–IR (ATR), υ_{max} (cm^{-1}): 3083–3030 (Ar–H), 2973 (Aliph. C–H), 2,232 (C≡N), 1661, 1574, 1449, 1332, 1266–1234–1171 (Ar–O–Ar), 1018, 965, 846, 763.

^{1}H NMR ($CDCl_3$), (δ:ppm): 7.97 (s, H, Ar–H), 7.78–7.67 (m, 4H, Ar–H), 7.51 (s, H, Ar–H), 7.13 (s, H, Ar–H), 6.57 (s, H, Ar–H), 2.51 (s, 3H, $-CH_3$).

^{13}C NMR ($CDCl_3$), (δ:ppm): 159.64, 156.59, 149.76, 145.48, 135.23, 133.91, 130.08, 129.29, 128.31, 127.79, 126.56, 125.59, 123.88, 122.98, 116.88 (C≡N), 115.23 (C≡N), 112.47, 19.02.

MALDI–TOF–MS *m*/z: Calculated for $C_{18}H_{11}N_3O$: 285.30; Found: 285.31 $[M]^+$.

2.1.2 | Quinoline-fused both peripheral and non-peripheral Zn^{II} (**ZnPc^{p}/ZnPc^{np}**) and Mg^{II} (**MgPc^{p}/MgPc^{np}**) phthalocyanines

CN^{p} or **CN^{np}** (0.1 g, 0.35 mmol) was solved in 1-pentanol (4 ml), after dissolution, related anyhdrous metal salt Zn $(OAc)_2$ (32 mg, 0.17 mmol) for the compounds (**ZnPc^{p}/ZnPc^{np}**) or $MgCl_2$ (17 mg, 0.17 mmol) for the compounds (**MgPc^{p}/MgPc^{np}**) was added into the reaction content. Then, DBU (six drops) was added dropwise slowly and the reaction mixture was continued with stirring at reflux temperature under N_2 atm, for day. The crude products precipitated with ethanol and filtered were purified by column chromatography upon aluminum oxide. Consequently, both peripheral and non-peripheral **ZnPc^{p}/ZnPc^{np}** and **MgPc^{p}/MgPc^{np}** were obtained as turquoise blue solids. The data of these phthalocyanines were given below.

*4-(4-methylquinolin-2-yloxy)phthalocyaninato zinc (II) (**ZnPc^{p}**)*
Yield: 40% (42 mg).
m.p. >300°C.
Solvent system of column chromatography: $CHCl_3$: C_2H_5OH (50:2 v/v).

FT–IR (ATR), υ_{max} (cm^{-1}): 3061 (Ar–H), 2922–2850 (Aliph. C–H), 1728, 1607, 1576, 1483, 1384, 1329, 1232, 1173, 1080, 946, 852, 743.

^{1}H NMR ($CDCl_3$), (δ:ppm): 7.90–7.26 (m, 32H, Ar–H), 2.70 (s, 12H, $-CH_3$).

UV–Vis (DMSO), λ_{max}, nm (logε): 678 (5.10), 612 (4.42), 353 (4.75).

MALDI–TOF–MS *m/z*: Calculated for $C_{72}H_{44}N_{12}O_4Zn$: 1206.59; Found: 1207.92 $[M + H]^+$.

*3-(4-methylquinolin-2-yloxy)phthalocyaninato zinc (II) (**ZnPc^{np}**)*
Yield: 36% (38 mg).
m.p. >300°C.
Solvent system of column chromatography: $CHCl_3$: C_2H_5OH (50:2 v/v).

FT–IR (ATR), υ_{max} (cm^{-1}): 3061 (Ar–H), 2921–2855 (Aliph. C–H), 1716, 1598, 1484, 1384, 1328, 1209, 1173, 1046, 982, 849, 751.

^{1}H NMR ($CDCl_3$), (δ:ppm): 7.91– 6.96 (m, 32H, Ar–H), 2.73 (s, 12H, $-CH_3$).

UV–Vis (DMSO), λ_{max}, nm (logε): 692 (5.05), 623 (4.38), 321 (4.62).

MALDI–TOF–MS *m/z*: Calculated for $C_{72}H_{44}N_{12}O_4Zn$: 1206.59; Found: 1207.86 $[M + H]^+$.

*4-(4-methylquinolin-2-yloxy)phthalocyaninato magnesium (II) (**MgPc^{p}**)*
Yield: 28% (28 mg).
m.p. >300°C.
Solvent system of column chromatography: $CHCl_3$: C_2H_5OH (50:2 v/v).

FT–IR (ATR), υ_{max} (cm^{-1}): 3061 (Ar–H), 2,924–2,855 (Aliph. C–H), 1717, 1645, 1599, 1482, 1384, 1331, 1269, 1174, 1080, 983, 850, 752.

^{1}H NMR ($CDCl_3$), (δ:ppm): 7.98–7.02 (m, 32H, Ar–H), 2.73 (s, 12H, $-CH_3$).

UV–Vis (DMSO), λ_{max}, nm (logε): 679 (4.99), 613 (4.36), 355 (4.71).

MALDI–TOF–MS *m/z*: Calculated for $C_{72}H_{44}N_{12}O_4Mg$: 1165.51; Found: 1166.86 $[M + H]^+$.

*3-(4-methylquinolin-2-yloxy)phthalocyaninato magnesium (II) (**MgPc^{np}**)*

Yield: 19% (19 mg).

m.p. >300°C.

Solvent of column chromatography: $CHCl_3$.

FT–IR (ATR), υ_{max} (cm^{-1}): 3061 (Ar–H), 2,922–2,846 (Aliph. C–H), 1728, 1605, 1575, 1446, 1384, 1328, 1231, 1173, 1109, 945, 851, 745.

^{1}H NMR ($CDCl_3$), (δ:ppm): 7.87–7.02 (m, 32H, Ar–H), 2.68 (s, 12H, $-CH_3$).

UV–Vis (DMSO), λ_{max}, nm (logε): 692 (5.01), 625 (4.33), 321 (4.56).

MALDI–TOF–MS *m/z*: Calculated for $C_{72}H_{44}N_{12}O_4Mg$: 1165.51; Found: 1170.89 $[M + 5H]^+$.

3 | RESULTS AND DISCUSSION

3.1 | Characterization of synthesized compounds

The general synthesis scheme of **CN^p/CN^{np}** and non-peripheral or peripheral quinoline-fused **ZnPc^p/ZnPc^{np}** and **MgPc^p/MgPc^{np}** is given in Scheme 1.

The structure of the new **CN^p/CN^{np}** was illuminated using MALDI-TOF mass, FT-IR, ^{13}C NMR, and ^{1}H NMR spectral data. Looking at the FT-IR spectra of **CN^p/CN^{np}**, the –OH stretching vibration of (**1**) at 3322 cm^{-1} disappeared and showed the typical C≡N stretching vibration at 2234 cm^{-1} (for **CN^p**), 2234 cm^{-1} (for **CN^{np}**). The

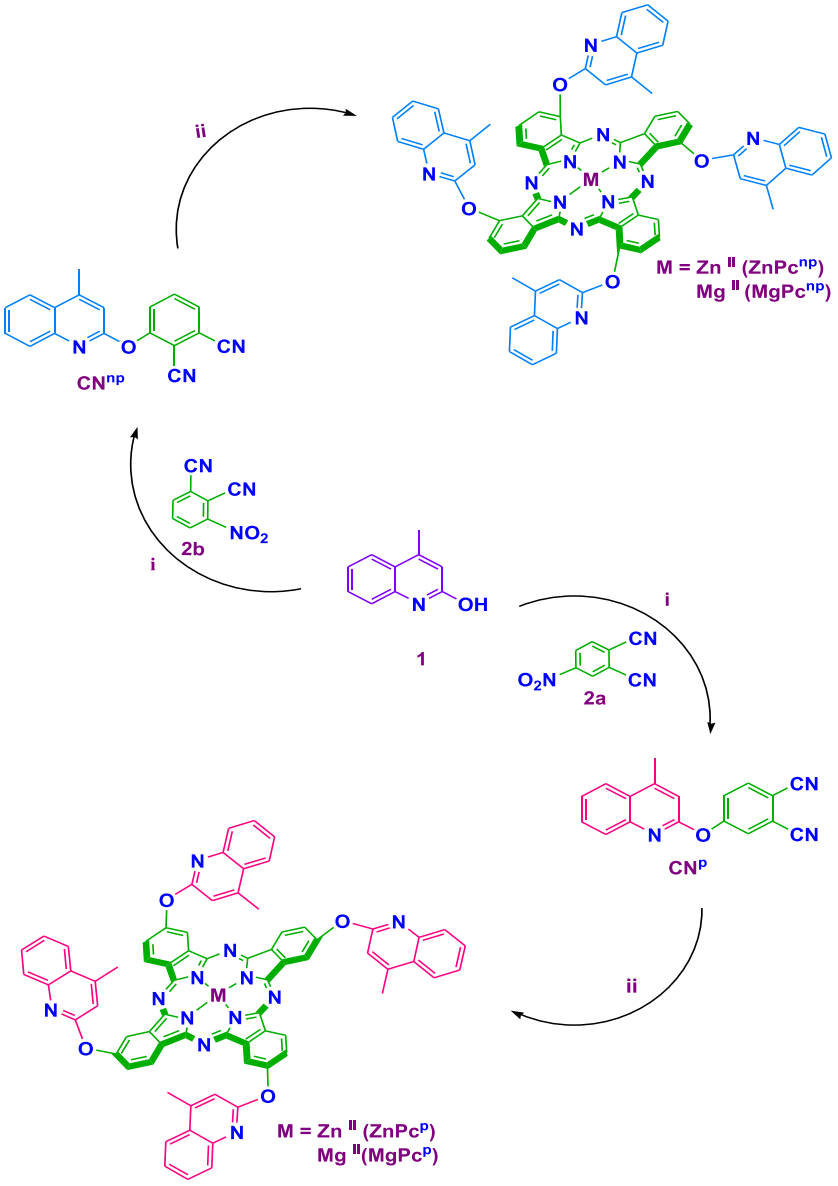

SCHEME 1 Synthesis scheme of quinoline-fused phthalonitrile derivatives and both non-peripheral and peripheral zinc (II) and magnesium (II) phthalocyanines (**CN^p/CN^{np}**, **ZnPc^p/ZnPc^{np}**, and **MgPc^p/MgPc^{np}**). Reagents and conditions (i) N_2, K_2CO_3, DMF, 56°C (ii) N_2, 1-pentanol, DBU, Zn $(OAc)_2$, $MgCl_2$, reflux temperature

^{1}H NMR and ^{13}C NMR spectra of the phthalonitrile derivatives (**CN^{p}/CN^{np}**) were recorded in $CDCl_3$. The aromatic protons of these compounds were exhibited among 7.98–6.59 ppm (for **CN^{p}**), 7.97–6.57 ppm (for **CN^{np}**) and also methyl group protons were exhibited at 2.52 ppm (for **CN^{p}**), 2.51 ppm (for **CN^{np}**). In the ^{13}C-NMR spectrum, the obtained phthalonitrile derivatives have characteristic peaks known as nitrile group (C≡N) and these peaks were observed between 116.87–116.45 ppm (for **CN^{p}**) and 116.88–115.23 ppm (for **CN^{np}**). The mass spectra of **CN^{p}/CN^{np}**, the molecular ion peaks were exhibited at *m*/*z*: 285.35 $[M]^+$ (for **CN^{p}**), 285.31 $[M]^+$ (for **CN^{np}**) (see Figure 1).

When the FT-IR spectra were examined for **ZnPc^{p}/ZnPc^{np}** and **MgPc^{p}/MgPc^{np}**, the typical C≡N stretching vibrations of the phthalonitriles were not observed. In addition to the structural elucidation of phthalonitrile compounds, the UV–Vis spectrum, which is an important spectroscopic method for Pc, was used for the structural elucidation of phthalocyanine compounds (Zn^{II}Pc and

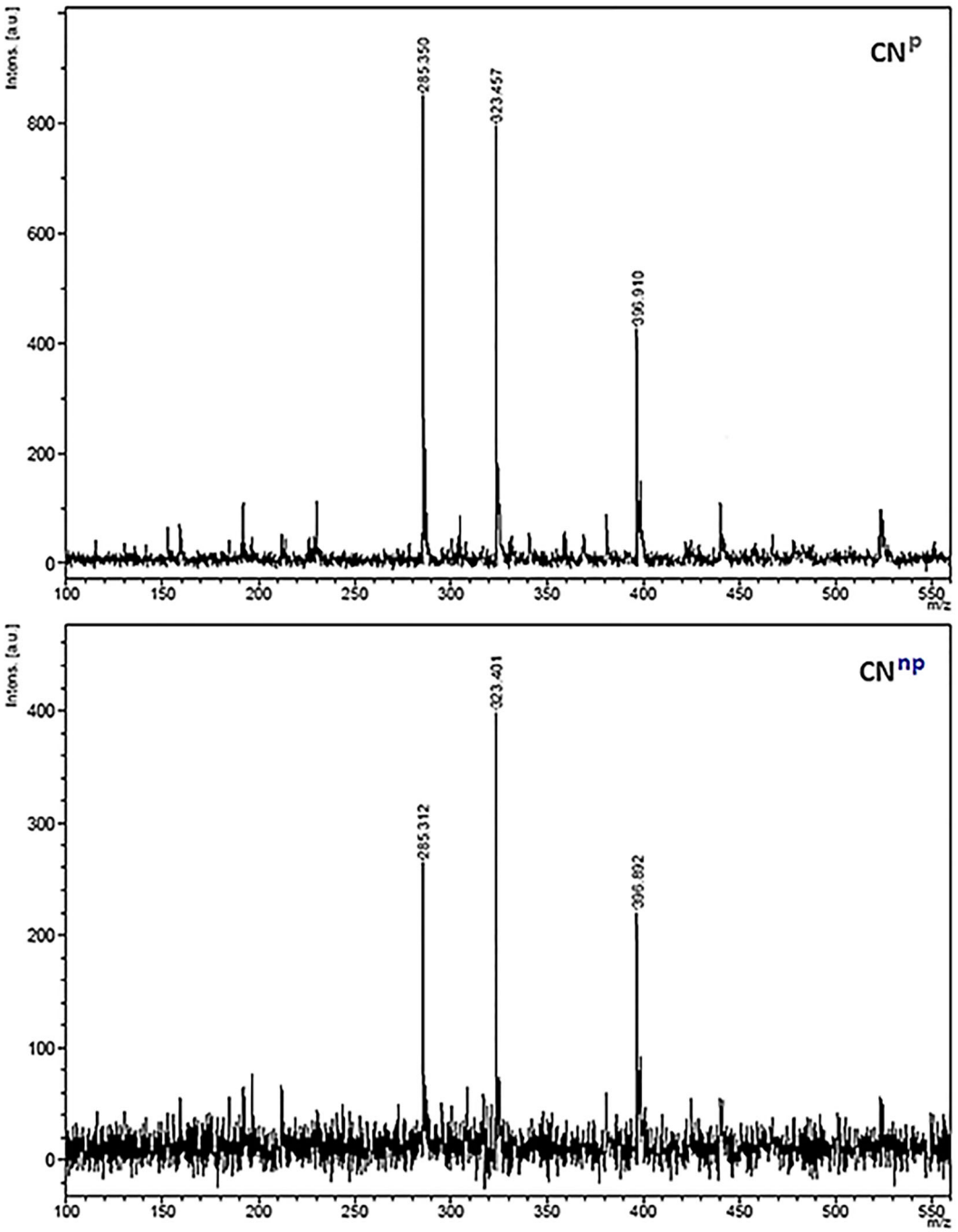

FIGURE 1 Mass spectra of quinoline-fused phthalonitrile derivatives (**CN^{p}/CN^{np}**)

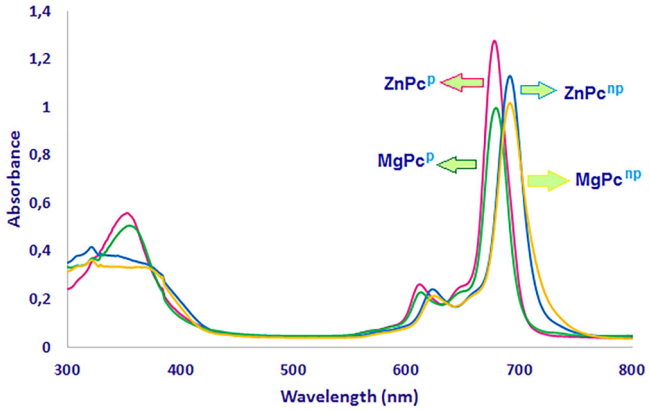

FIGURE 2 UV–Vis spectra of quinoline-fused both non-peripheral and peripheral Zn^{II} and Mg^{II} phthalocyanines (**$ZnPc^{p}$/$ZnPc^{np}$** and **$MgPc^{p}$/$MgPc^{np}$**) in DMSO (C:1 × 10^{-5} M)

Mg^{II}Pc). In the UV–Vis spectrum, which is one of the most important indicators of the formation of phthalocyanines, Pcs have two absorption bands known as Q and B bands. The UV–Vis spectra of **$ZnPc^{p}$/$ZnPc^{np}$** and Mg^{II} **$MgPc^{p}$/$MgPc^{np}$** phthalocyanines were recorded in DMSO at a concentration of 1.0 × 10^{-5} M and also these compounds were observed Q bands at approximately 692–678 nm and B bands among 355–321 nm (see Figure 2). When the mass spectra of phthalocyanines were analyzed, the molecular ion peaks were exhibited at *m*/*z* values of 1207.92 $[M + H]^+$ (**$ZnPc^{p}$**), 1207.86 $[M + H]^+$ (**$ZnPc^{np}$**), 1166.86 $[M + H]^+$ (**$MgPc^{p}$**), and 1170.89 $[M + 5H]^+$ (**$MgPc^{np}$**) (see Figure 3).

3.2 | Biological activities

Alzheimer's disease is a common type of dementia, a progressive neurological disease that causes the destruction of brain cells. In this disease, symptoms of a decrease in thought, memory, and behavioral functions occur. Cholinesterase inhibition is one of the most commonly used strategies in the treatment of this disease.[52,53] In this paper, in vitro cholinesterases inhibitory effects of the compounds were examined using spectrophotometer methods. The IC_{50} and selective index (SI) values of the compounds on cholinesterases were given in Table 1. In this work, galantamine was used as a positive control. **$MgPc^{np}$** showed the highest inhibitory actions with IC_{50} values of 25.16 ± 1.27 and 30.02 ± 3.00 μM on AChE and BuChE, but it had lower inhibitory effects than galantamine used as a positive control. The SI value of **$MgPc^{np}$** was 1.19. Also, the IC_{50} values of **$ZnPc^{p}$** against AChE and BuChE were determined as 32.01 ± 3.58 and 33.81 ± 1.73 μM. Among these compounds, it was revealed that the non-peripheral compound showed the highest inhibitory properties. It is known that the most fundamental problems of phthalocyanines are solubility and aggregation. However, this situation can be overcome thanks to non-peripheral compounds.[54] Higher inhibitory efficacy of non-peripheral compound may be due to low aggregation and high solubility. There are literatures that magnesium is associated with Alzheimer's disease by inhibiting the cholinesterase enzyme. For this reason, it is thought that the magnesium phthalocyanine compound has a higher effect.[55]

DM is a disease that develops due to high blood sugar, which occurs as a result of the pancreas's inability to produce enough insulin for the body or the body's inability to use the insulin it produces effectively. Glucosidase inhibitors play an important role in the treatment of this disease. Since the glucosidase inhibitors used have side effects, the search for alternative molecules continues.[56,57] In this paper, in vitro α-glucosidase inhibitory properties of the compounds were investigated using spectrophotometer methods. The IC_{50} values of the compounds on α-glucosidase were presented in Table 2. Acarbose was used as a positive control. **$MgPc^{np}$** showed the best inhibitory properties with IC_{50} values of 27.31 ± 9.44 on α-glucosidase, but it had 1.85 fold higher inhibitory effects than acarbose which used as a positive control. The IC_{50} values of **$MgPc^{np}$**, **$ZnPc^{np}$**, and **$ZnPc^{p}$** were 35.37 ± 2.31, 37.27 ± 2.60, and 46.71 ± 7.47 μM. In recent years, there have been few literatures on cholinesterase and α-glucosidase inhibition studies of metal complexes. Günsel et al. reported that the IC_{50} values of 1-methyl-1H-imidazole-2-thiol substituents zinc (II) phthalocyanines was 92.31 μM and 24.37 μM on AChE and BuChE.[58] In another study, Şenocak et al. reported that the IC_{50} values of amino acid Schiff base Zn (II) complexes ranged from 9.61 to 35.57 μM on AChE, BuChE, and α-glucosidase.[59] Sarria et al. reported cholinesterase inhibitory properties of zinc (II) complexes with flavanone derivatives (hesperidin, hesperetin, naringin, and naringenin). The results showed that metal complexes-flavanone had noticeable inhibitory actions on cholinesterase enzymes.[60] Avcı et al. investigated α-glucosidase inhibitory properties of 6-methylpyridine-2-carboxylic acid and 2,2′-dipyridlamine substituted copper (II), cobalt (III), and zinc (II) complexes. The results showed that while ligands alone did not show activity, inhibition was observed in the presence of copper (II) metal.[61]

One of the main causes of cancer is thought to be damage to DNA. Therefore, in many studies, preliminary data can be obtained on whether the compounds are toxic through DNA damage.[62–65] Therefore, it was investigated whether the compounds cause DNA damage in this study. DNA hydrolytic nuclease experiments of the

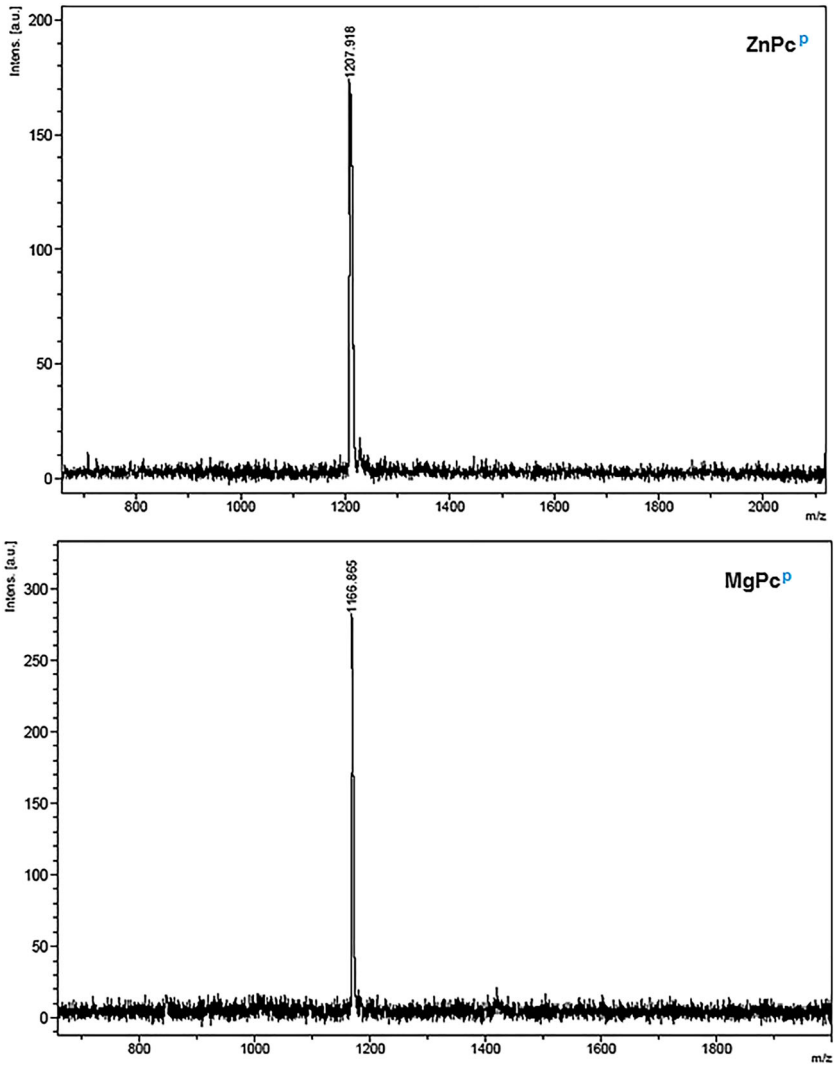

FIGURE 3 Mass spectra of quinoline-fused peripheral Zn^{II} and Mg^{II} phthalocyanines (**$ZnPc^p$** and **$MgPc^p$**)

TABLE 1 IC_{50} (μM) and SI (BuChE/AChE) values of the compounds on AChE, BuChE

	AChE	BuChE	SI value (BuChE/AChE)
$ZnPc^p$	32.01 ± 3.58	33.81 ± 1.73***	1.06
$MgPc^p$	58.86 ± 7.10	36.33 ± 2.12*	0.62
$ZnPc^{np}$	37.74 ± 9.34	55.23 ± 1.93	1.46
$MgPc^{np}$	25.16 ± 1.27	30.02 ± 3.00***	1.19
Galantamine	21.04 ± 0.08	43.58 ± 0.20	2.07

*$p < 0.05$. ***$p < 0.0001$ compared to positive control.

compounds were measured using agarose gel electrophoresis on supercoiled plasmid pBR322 DNA. The results were presented in Figure 4. Plasmid DNA can be seen in three different forms on agarose gel (Sc form: supercoiled form, Nc form: nicked form, Lc form: linear form). The results showed that Sc form was found to be approximately 90% (Figure 1, lane 1) without any compounds. On the addition of all compounds at 25 and 50 μM, the percentage of Sc of DNA did not change. The results revealed that the compounds did not cause plasmid DNA damage at the concentrations used. As it is known, phthalocyanines have low toxicity at low concentrations in the dark. Therefore, it may not have shown DNA damage.

Antioxidants prevent cell damage by scavenging the damaging biomolecules called free radicals in our cells. The DPPH method is one of the most commonly used antioxidant methods because it is reliable, fast, and inexpensive.[66,67] In this study, DPPH radical scavenging effects of the compounds were investigated using

TABLE 2 α-Glucosidase inhibitory effects and DPPH radical scavenging inhibitory actions of the compounds

	α-Glucosidase	DPPH
ZnPc^{p}	46.71 ± 7.47	>100
MgPc^{p}	27.31 ± 9.44***	>100
ZnPc^{np}	37.27 ± 2.60*	>100
MgPc^{np}	35.37 ± 2.31*	>100
Acarbose	50.44 ± 0.50	—
Gallic acid	—	20.48 ± 0.20

*$p < 0.05$. ***$p < 0.0001$ compared to positive control.

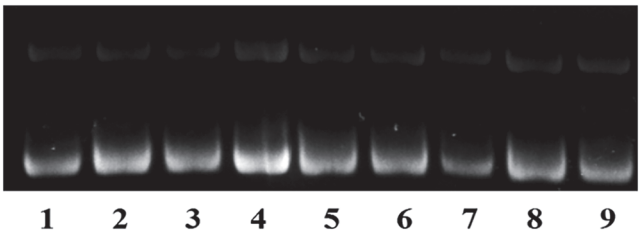

FIGURE 4 DNA hydrolytic nuclease effects of the compounds. Lane 1: DNA control; lane 2–3: (25 and 50 μM of **ZnPc^{p}**); lane 4–5: (25 and 50 μM of **MgPc^{p}**); lane 6–7: (25 and 50 μM of **ZnPc^{np}**); lane 8–9: (25 and 50 μM of **MgPc^{np}**)

spectrophotometric methods. Gallic acid was used as a positive control. The results indicated that SC_{50} values of the compounds are greater than 100 μM. On the other hand, the SC_{50} value of gallic acid was calculated as 20.48 ± 0.20 μM. These results revealed that the compounds did not have radical scavenging activities.

3.3 | In silico calculations

Theoretical calculations allow to interpret the activities of compounds without any experimental procedure. Theoretical calculations explain many important properties of compounds. First, the quantum chemical parameters compounds are calculated with of the Gaussian package program. With these calculations, the numerical value of the parameters of the compounds is taken into account in order to predict the activities of the compounds.[15,16]

The two parameters checked to compare the activities of compounds are the highest-occupied molecular orbital (HOMO) and the lowest-unoccupied molecular orbital (LUMO) of the compounds. These two parameters are used to explain the chemical activities of compounds. The numerical value of the HOMO parameter of the compounds shows the electron accepting ability of the compounds. The compound with the higher HOMO energy value has higher activity than the others.[68] Because it has the ability to donate electrons more easily.[69] On the other hand, the LUMO energy value of compounds indicates the ability of compounds to accept electrons into vacant orbitals. The compound with the lower LUMO energy value has higher activity than the other compound. Because it has the ability to accept electrons more easily.[68] By examining these two parameters, they are used to explain the activities of compounds with their ability to donate electrons.Another parameter is the ΔE energy gap, which is equal to the energy value difference between the HOMO and LUMO parameters of the compounds.[69] The activity of the compound with the lowest numerical value of this parameter is higher than the other compounds. Therefore, the low numerical value of this parameter indicates that less energy should be required for the electron in the HOMO to pass to the vacant orbitals in the LUMO.[15] Therefore, less energy causes this transition to be easier. This is another important parameter that determines the activity of the compound. Although many quantum chemical parameters are calculated as a result of the calculations, most of the calculated parameters are calculated from the numerical values of the HOMO and LUMO parameters. Therefore, the ordering in other parameters is similar to the ordering in HOMO and LUMO.

In the calculations of **CN^{p}/CN^{np}**, **ZnPc^{p}/ZnPc^{np}**, and **MgPc^{p}/MgPc^{np}** with the Gaussian program, it is seen that the **MgPc^{np}** has a higher HOMO value in other compounds and metallated phthalocyanine compounds. On the other hand, it was observed that the compound with the lowest ΔE energy value was **MgPc^{np}**. As a result of the calculations, in general, the **MgPc^{np}** has a higher activity to the Gaussian program than other compounds and metallated phthalocyanines.

Visual representations of some of the calculated quantum chemical parameters of the compounds are available. Figure 5 shows the visuals of these parameters. The first visualization of **CN^{p}/CN^{np}** in Figure 5 and their optimized structures of **ZnPc^{p}/ZnPc^{np}** and **MgPc^{p}/MgPc^{np}** are given. In the second and third images, HOMO and LUMO images of the compounds are given, which shows on which atoms the HOMO and LUMO orbitals are located. In the last image, the representation of the electrostatic potentials of the compounds is given. In this image, it is given on which atoms the electrons in the compound are concentrated. If this electron density is high, it is shown in red.[69] On the other hand, if this electron density is low, it is shown in blue other regions are shown in green. Both the red colored regions and the blue colored regions are the regions with high activity of the compound. Because electron-rich regions can interact by donating electrons.[15] On the other hand, electron-

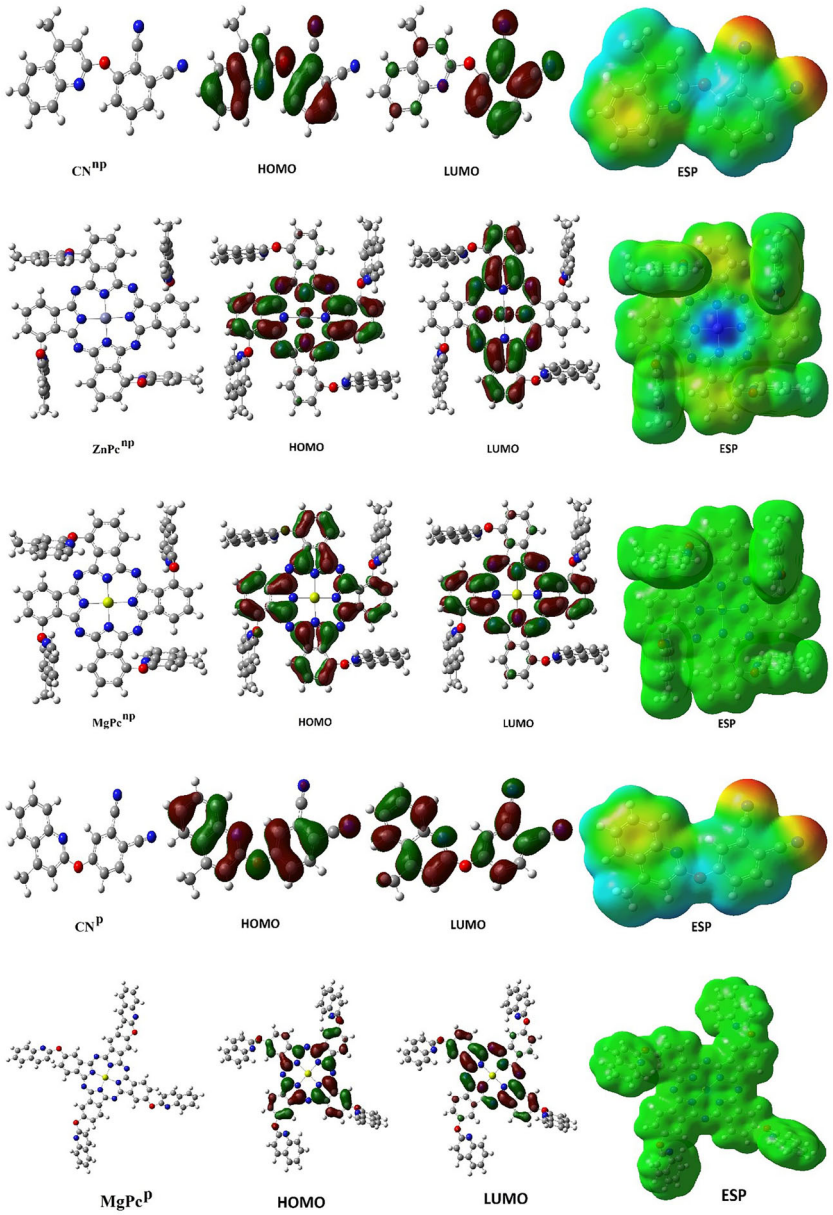

FIGURE 5 Representations of optimize structure, HOMO, LUMO, and ESP of phthalonitrile derivatives (**CN^{p}/CN^{np}**) and Zn^{II} (**ZnPc^{p}/ZnPc^{np}**) and Mg^{II} (**MgPc^{p}/MgPc^{np}**) phthalocyanine compounds

poor blue regions are regions with a high probability of accepting electrons and interacting.[16] Therefore, this figure in which electrostatic potentials are shown is very important for the activity of the compound.

Quantum chemical parameters alone are not sufficient to compare the activities of compounds. Molecular docking calculations are performed to compare the activities of compounds against cancer proteins. Many parameters are calculated with these calculations. All calculated parameters are given in Table 3. Among these parameters is the E total energy parameter, which is used to compare the activities of compounds. It is known that the activity of the compound with the most negative value for this parameter has higher activity than other compounds.[70] The most important factor determining the activity of the compound is the chemical interaction of the compound with the cancer proteins. Compound with higher chemical interaction energy has higher activity than other compounds.[59,71] Therefore, the chemical interaction of the compound is very important for the activity. These chemical interactions between the compound and cancer proteins are hydrogen bonds, polar and hydrophobic interactions, π–π, and halogen.[72] The interactions of molecules with cancer proteins and the parameters obtained from this interaction are given in Table 3 and Figures 6–9.

When the interactions of **CN^{p}/CN^{np}**, **ZnPc^{p}/ZnPc^{np}**, and **MgPc^{p}/MgPc^{np}** with cancer proteins were examined, comparisons to E total energy values were made.[73] In the calculations made, it was seen that the biological activity of the phthalonitrile derivatives was lower than that of the metallated phthalocyanine compounds.

TABLE 3 The calculated quantum chemical parameters of compounds

	E_{HOMO}	E_{LUMO}	I	A	ΔE	η	μ	χ	Pİ	ω	ε	dipol	Energy
B3LYP/6-31g LEVEL													
CN^{np}	−6.6336	−2.1239	6.6336	2.1239	4.5098	2.2549	0.4435	4.3788	−4.3788	4.2515	0.2352	9.2613	−25348.8467
$ZnPc^{np}$	−4.7762	−2.6145	4.7762	2.6145	2.1617	1.0808	0.9252	3.6953	−3.6953	6.3171	0.1583	0.0051	−149813.6003
$MgPc^{np}$	−4.7579	−2.6183	4.7579	2.6183	2.1396	1.0698	0.9347	3.6881	−3.6881	6.3572	0.1573	0.0040	−106846.6837
CN^{p}	−6.6328	−2.1636	6.6328	2.1636	4.4692	2.2346	0.4475	4.3982	−4.3982	4.3283	0.2310	10.437	−25348.9050
$ZnPc^{p}$	−5.2026	−2.9990	5.2026	2.9990	2.2036	1.1018	0.9076	4.1008	−4.1008	7.6314	0.1310	0.0005	−145537.6932
$MgPc^{p}$	−5.1835	−3.0033	5.1835	3.0033	2.1802	1.0901	0.9173	4.0934	−4.0934	7.6857	0.1301	0.0177	−102570.7890
HF/6-31g LEVEL													
CN^{np}	−8.8286	1.4871	8.8286	−1.4871	10.3158	5.1579	0.1939	3.6708	−3.6708	1.3062	0.7656	9.4678	−25188.5431
$ZnPc^{np}$	−5.3531	0.0204	5.3531	−0.0204	5.3735	2.6867	0.3722	2.6663	−2.6663	1.3230	0.7558	3.7615	−149125.2886
$MgPc^{np}$	−5.3400	0.0245	5.3400	−0.0245	5.3645	2.6822	0.3728	2.6578	−2.6578	1.3167	0.7594	4.0563	−106189.4497
CN^{p}	−8.8283	1.4428	8.8283	−1.4428	10.2710	5.1355	0.1947	3.6928	−3.6928	1.3277	0.7532	10.696	−25188.6043
$ZnPc^{p}$	−5.4401	−0.0623	5.4401	0.0623	5.3778	2.6889	0.3719	2.7512	−2.7512	1.4075	0.7105	4.3342	−144881.5076
$MgPc^{p}$	−5.3944	−0.0169	5.3944	0.0169	5.3776	2.6888	0.3719	2.7056	−2.7056	1.3613	0.7346	4.4617	−101945.6407
M062X/6-31g LEVEL													
CN^{np}	−6.6336	−2.1239	6.6336	2.1239	4.5098	2.2549	0.4435	4.3788	−4.3788	4.2515	0.2352	6.6284	−25338.9242
$ZnPc^{np}$	−5.7267	−2.2409	5.7267	2.2409	3.4858	1.7429	0.5738	3.9838	−3.9838	4.5529	0.2196	2.0917	−149774.0404
$MgPc^{np}$	−5.6978	−2.2395	5.6978	2.2395	3.4583	1.7292	0.5783	3.9687	−3.9687	4.5543	0.2196	0.0025	−106807.6280
CN^{p}	−7.9439	−1.2305	7.9439	1.2305	6.7134	3.3567	0.2979	4.5872	−4.5872	3.1344	0.3190	10.241	−25338.9985
$ZnPc^{p}$	−6.0206	−2.5154	6.0206	2.5154	3.5051	1.7526	0.5706	4.2680	−4.2680	5.1969	0.1924	0.0117	−145499.8095
$MgPc^{p}$	−5.9895	−2.5144	5.9895	2.5144	3.4752	1.7376	0.5755	4.2519	−4.2519	5.2023	0.1922	0.0180	−102533.4661

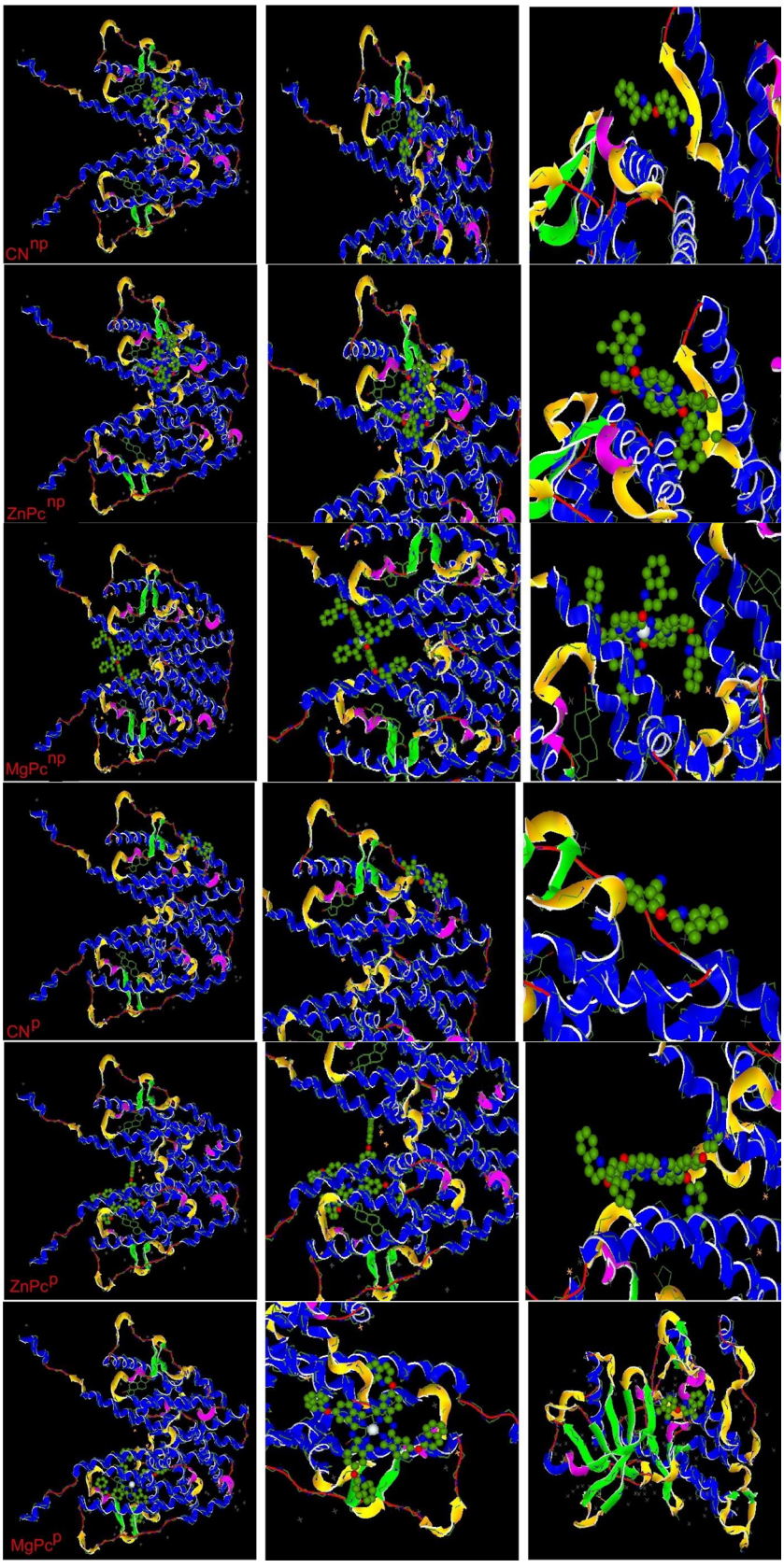

FIGURE 6 Demonstration of molecular interactions all compounds with breast cancer

However, for a more detailed analysis, chemical interaction was revealed by PLIP analysis. All chemical interactions are given in Tables 4–7. The interaction of the **ZnPc^{p}** with the highest activity as a result of the docking calculations was examined in detail and given in Figures 10–13.

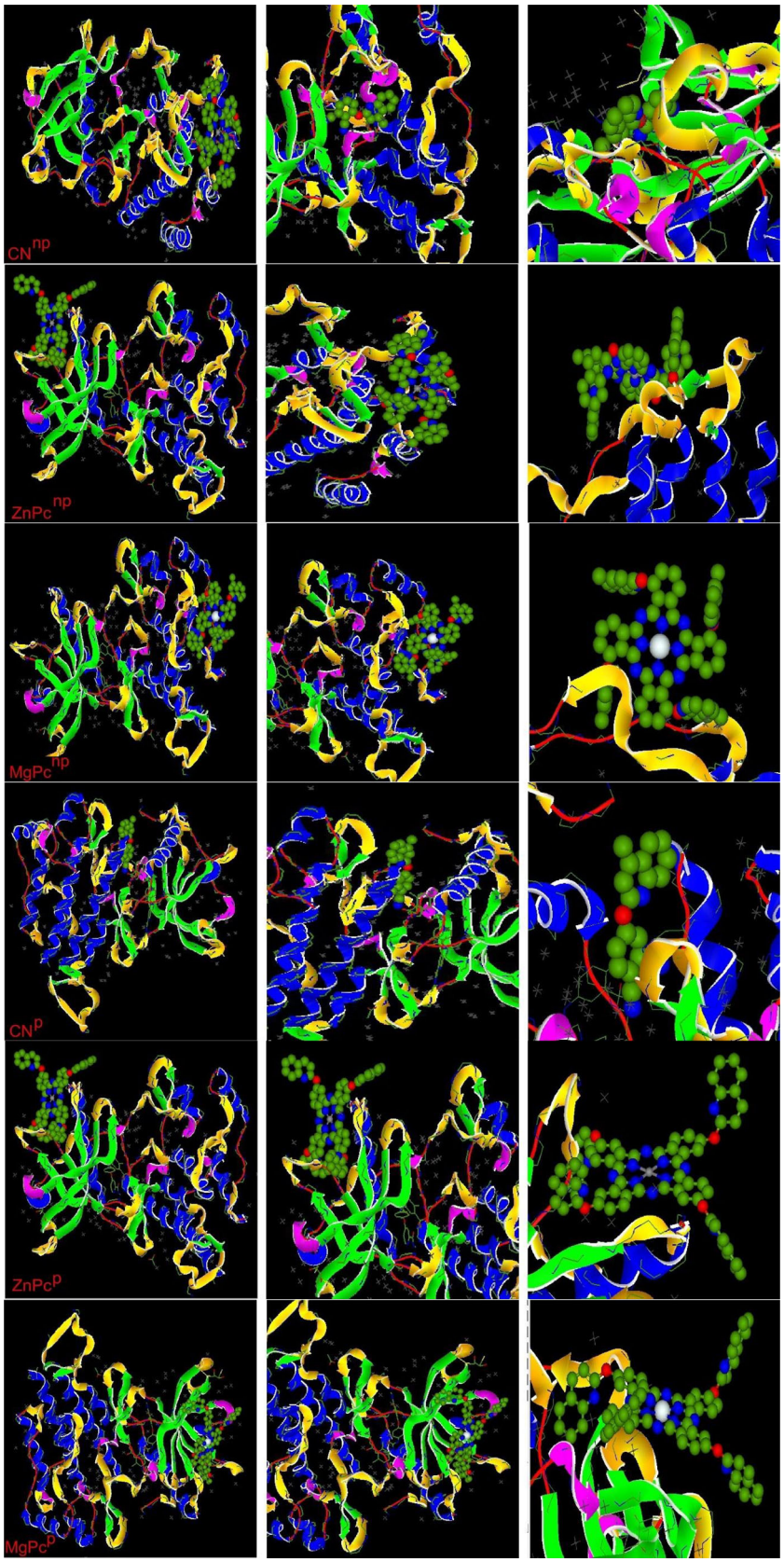

FIGURE 7 Demonstration of molecular interactions all compounds with liver cancer

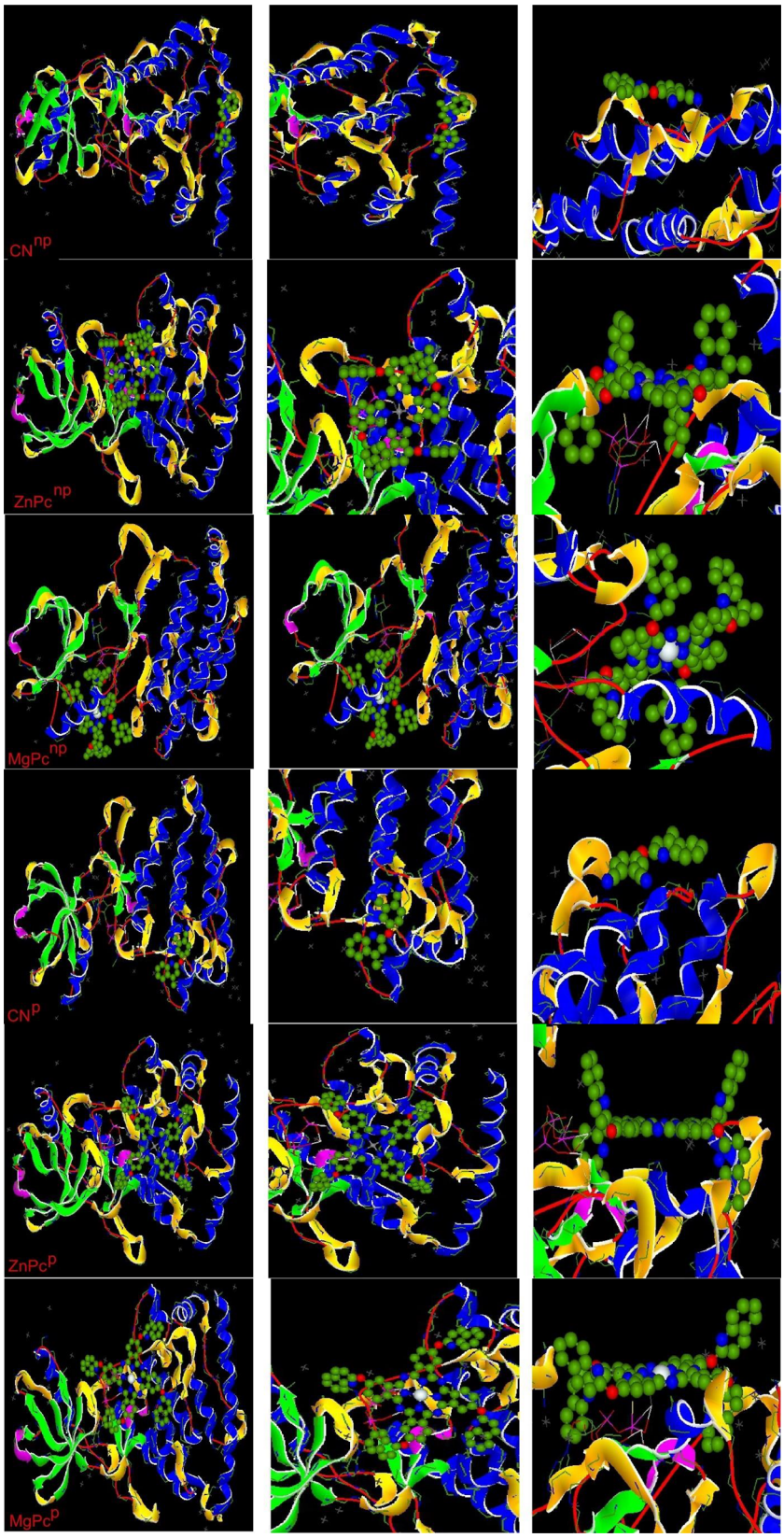

FIGURE 8 Demonstration of molecular interactions all compounds with colon cancer

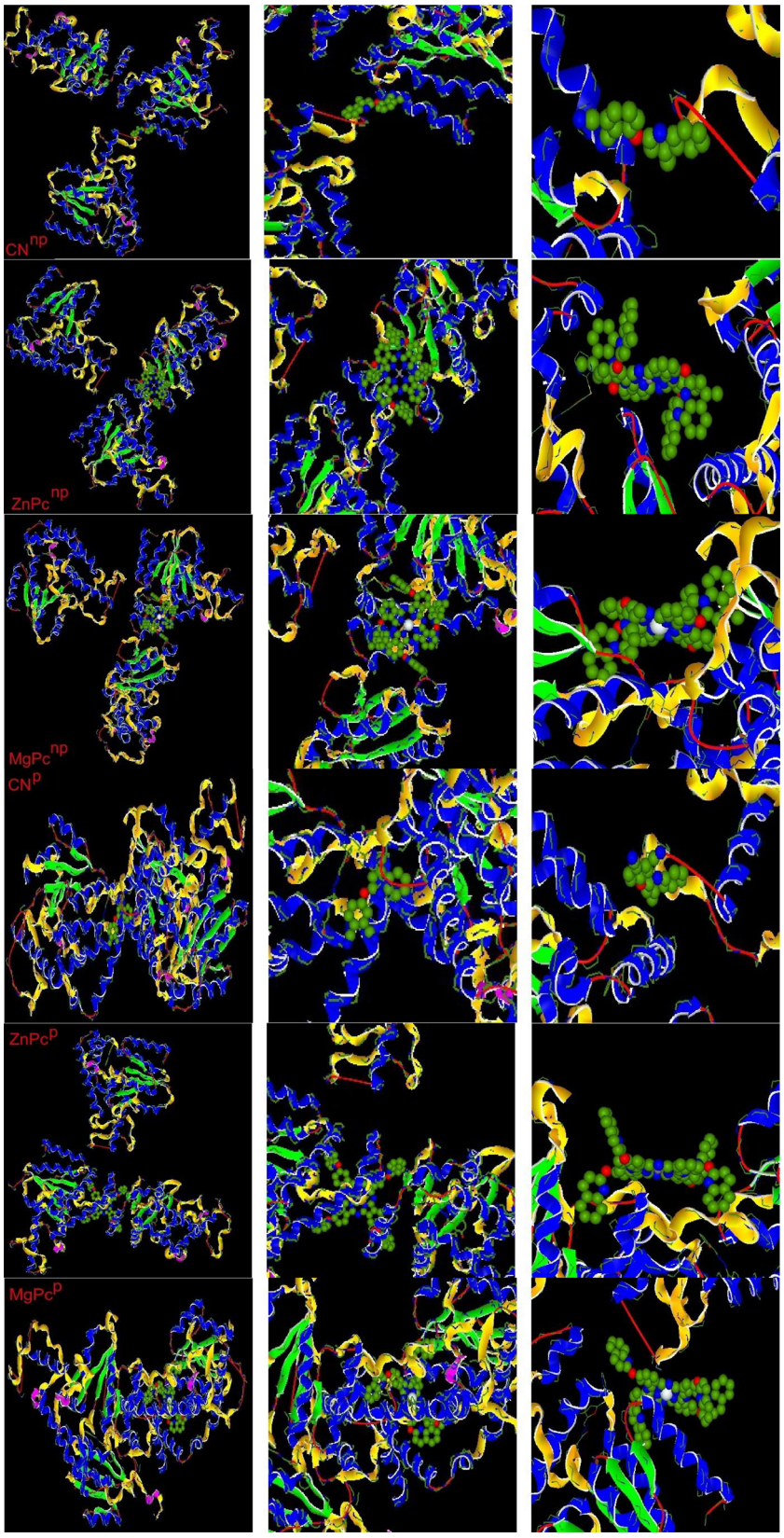

FIGURE 9 Demonstration of molecular interactions all compounds with lung cancer

TABLE 4 E total energy values of compounds against protein

	Breast cancer	Liver cancer	Colon cancer	Lung cancer
CN^{np}	−280.14	−251.87	−241.52	−241.12
$ZnPc^{np}$	−434.16	−328.25	−446.12	−452.19
$MgPc^{np}$	−433.44	−378.24	−425.99	−448.47
CN^{p}	−286.39	−253.29	−249.86	−241.95
$ZnPc^{p}$	−566.25	−453.26	−485.22	−477.77
$MgPc^{p}$	−479.13	−450.87	−457.26	−447.63

TABLE 5 Hydrophobic Interactions of proteins and **$ZnPc^{p}$** phthalocyanine compound

Index	Residue	AA	Distance	Ligand atom	Protein atom
Breast cancer-$ZnPc^{p}$					
1	380A	GLU	3.18	4771	708
2	422B	VAL	3.96	4723	3421
3	422B	VAL	3.75	4725	3423
4	423B	GLU	3.96	4714	3429
5	426B	ASP	3.88	4693	3460
6	429B	LEU	3.18	4756	3487
7	430B	ALA	3.63	4755	3496
8	460A	THR	3.29	4705	1475
9	462A	LEU	3.77	4696	1496
Liver cancer-$ZnPc^{p}$					
1	869A	MET	3.59	3221	532
2	870A	LEU	3.47	3154	541
3	875A	THR	2.77	3211	586
4	883A	MET	1.76	3184	687
5	908A	PRO	3.85	3176	922
6	911A	PRO	2.87	3150	938
Colon cancer proteins-$ZnPc^{p}$					
1	207A	ALA	3.86	2531	661
2	213A	ALA	3.14	2551	719
3	263A	ASP	3.76	2586	1038
4	307A	ALA	3.55	2508	1300
5	342A	VAL	3.74	2485	1632
6	348A	ASP	3.67	2563	1680
Lung cancer proteins-$ZnPc^{p}$					
1	277A	GLU	3.46	7218	2502
2	281A	ILE	3.46	7322	2537
3	281A	ILE	3.95	7315	2538
4	283A	HIS	3.87	7244	2556
5	289A	THR	3.07	7225	2610
6	504A	VAL	3.05	7278	4436
7	514B	ASN	3.75	7287	2133
8	516B	PRO	2.93	7289	2154

TABLE 6 Hydrogen Bonds of proteins and **ZnPc^{p}** phthalocyanine compound

Index	Residue	AA	Distance H-A	Distance D-A	Donor angel	Protein donor?	Side chain	Donor Atom	Acceptor Atom
Breast cancer-ZnPc^{p}									
1	416B	LYS	2.74	3.31	114.37	√	√	3373 [N3+]	4743 [O2]
2	426B	ASP	2.65	3.33	129.77	√	√	3463 [O3]	4697 [N2]
3	520B	LYS	2.28	2.76	106.16	√	√	4400 [N3+]	4745 [O2]
Liver cancer-ZnPc^{p}									
1	870A	LEU	3.17	3.57	105.52	√	√	537 [Nam]	3171 [O2]
2	873A	GLY	3.32	3.80	111.65	√	√	569 [Nam]	3172 [O2]
3	876A	HIS	3.63	4.06	108.96	√	√	589 [Nam]	3148 [N2]
4	876A	HIS	3.28	4.07	136.26	√	√	595 [Nar]	3138 [N2]
5	879A	HIS	2.98	3.78	137.70	√	√	631 [Nar]	3128 [N2]
Colon cancer-ZnPc^{p}									
1	209A	ASN	1.99	2.55	113.12	√	√	679 [Nam]	2493 [N2]
2	265A	LYS	3.54	4.04	111.95	√	√	1060 [N3+]	2593 [N2]
3	267A	SER	3.16	4.00	149.52	√	√	1078 [O3]	2483 [N2]
Lung cancer-ZnPc^{p}									
1	283A	HIS	2.96	3.78	139.90			2558 [Nar]	7222 [N2]
2	289A	THR	2.96	3.90	172.76			2609 [O3]	7219 [Nar]
3	293A	ARG	2.37	2.98	117.48			2642 [N3]	7268 [O2]

TABLE 7 π-cation interactions of proteins and **ZnPc^{p}** phthalocyanine compound

Index	Residue	AA	Distance	Offset	Protein charged?	Ligand Group	Ligand Atoms
Liver cancer-ZnPc^{p}							
1	879A	HIS	3.66	1.31	√	Aromatic	3121, 3122, 3125, 3126, 3127
2	879A	HIS	3.53	0.89	√	Aromatic	3119, 3120, 3121, 3122, 3123, 3124
Lung cancer-ZnPc^{p}							
1	283A	HIS	2.44	0.18	√	Aromatic	7243, 7244, 7245, 7246, 7247, 7248

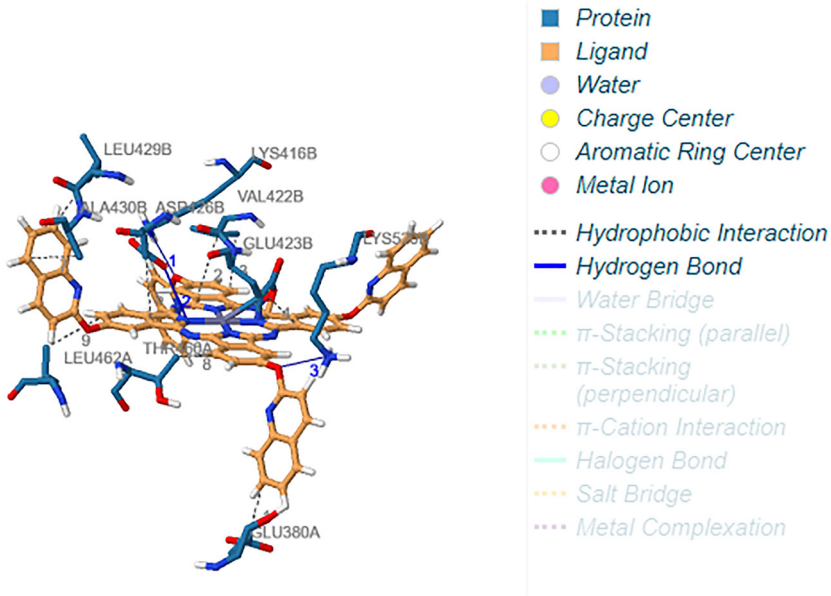

FIGURE 10 Demonstration of interactions between **ZnPc^{p}** phthalocyanine compound and breast cancer protein

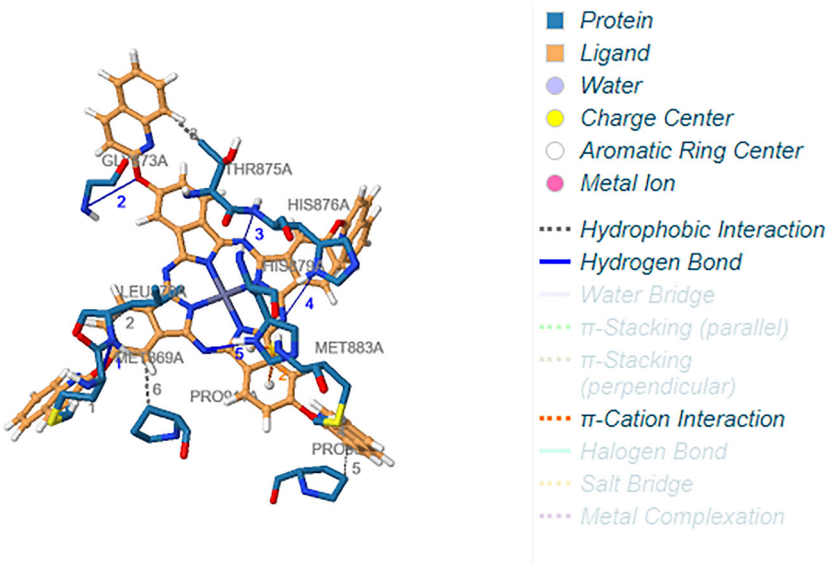

FIGURE 11 Demonstration of interactions between **ZnPc^{p}** phthalocyanine compound and liver cancer protein

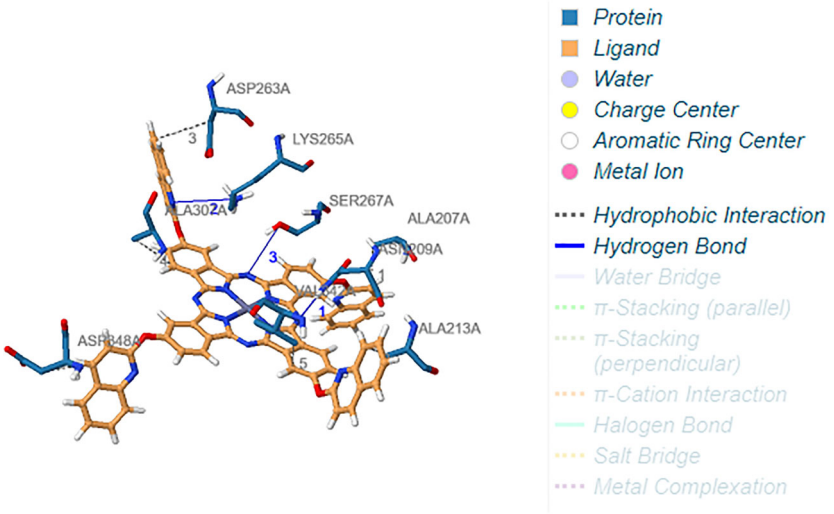

FIGURE 12 Demonstration of interactions between **ZnPc^{p}** phthalocyanine compound and colon cancer protein

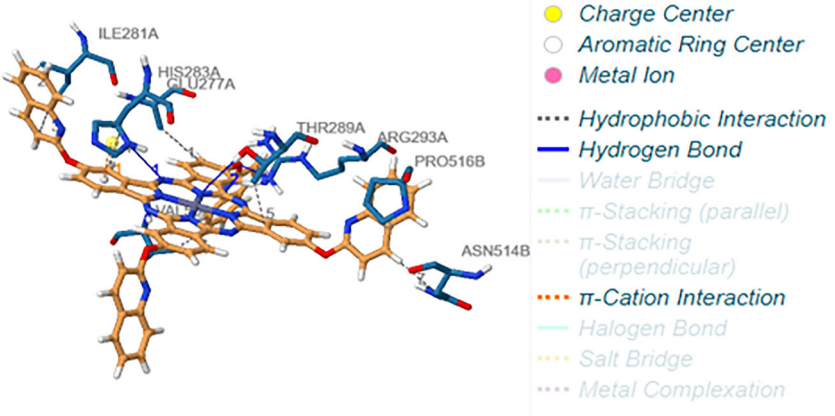

FIGURE 13 Demonstration of interactions between **ZnPc^{p}** phthalocyanine compound and lung cancer protein

4 | CONCLUSION

In this study, quinoline-fused **ZnPc^{p}/ZnPc^{np}** and **MgPc^{p}/MgPc^{np}** were elucidated by various spectroscopic methods, were synthesized and their biological activities were investigated. The **MgPc^{np}** compound has the best inhibitory effect on AChE and BuChE among the tested compounds, with IC50 values of 25.16 ± 1.27 and 30.02 ± 3.00 μM. In addition, **MgPc^{p}** compound was found to have the highest α-glucosidase inhibition effect with 27.31 ± 9.44 μM. The peripheral or non-peripheral **ZnPc^{p}/ZnPc^{np}** and **MgPc^{p}/MgPc^{np}** phthalocyanines showed no damage to the supercoiled plasmid pBR322 DNA at 25 and 50 μM, suggesting that the compounds have a low toxic effect. The theoretical calculations made, both chemical and biological activities of all compounds were examined. When the activities of **CN^{p}/CN^{np}**, **ZnPc^{p}/ZnPc^{np}**, and **MgPc^{p}/MgPc^{np}** are compared by examining their chemical properties, it is seen that the **MgPc^{np}** with HOMO energy value of −4.7579 at B3LYP level and −5.3400 at Hf level has higher activity than other compounds. Although chemical activity calculations examine the compound pure and isolated, biological activity calculations examine the activities of compounds against different cancer proteins. When the interaction with different cancer proteins is examined, it is seen that **ZnPc^{p}** is higher than other molecules against cancer proteins.

ACKNOWLEDGMENTS

The numerical calculations reported in this paper were fully/partially performed at TUBITAK ULAKBIM, High Performance and Grid Computing Center (TRUBA resources).

AUTHOR CONTRIBUTIONS

Halise Yalazan: Investigation; methodology. **Burak Tüzün:** Funding acquisition; methodology. **Didem Akkaya:** Investigation. **Burak Barut:** Investigation. **Halit Kantekin:** Methodology; supervision. **Sermet Yıldırmış:** Investigation.

ORCID

Halise Yalazan https://orcid.org/0000-0003-1234-2721
Burak Tüzün https://orcid.org/0000-0002-0420-2043
Didem Akkaya https://orcid.org/0000-0002-0711-951X
Burak Barut https://orcid.org/0000-0002-7441-8771
Halit Kantekin https://orcid.org/0000-0003-2625-2815
Sermet Yıldırmış https://orcid.org/0000-0001-7535-5912

REFERENCES

[1] E. N. Barut, B. Barut, S. Engin, S. Yıldırım, A. Yaşar, S. Turkis, A. Özel, F. S. Sezen, *Turkish J. Biochem.* **2017**, *42*, 493.
[2] H. M. Ragaba, M. Teleba, H. R. Haidarb, N. Gouda, *Bioorg. Chem.* **2019**, *86*, 557.
[3] M. S. A. Rawa, Z. Hassan, V. Murugaiyah, T. Nogawa, H. A. Wahab, *J. Ethnopharmacol.* **2019**, *245*, 112160.
[4] T. Arslan, M. B. Ceylan, H. Baş, Z. Biyiklioglu, M. Senturk, *Dalton Trans.* **2020**, *49*, 203.
[5] J. A. Lima, T. W. R. Costa, A. C. C. Fonseca, R. F. Amaral, M. D. S. B. Nascimento, O. A. Santos-Filho, A. L. Miranda, D. C. F. Neto, F. R. S. Lima, L. Hamerski, L. W. Tinoco, *Bioorg. Chem.* **2020**, *104*, 104,215.
[6] S. Shaikha, P. Dhavanb, G. Pavalea, M. M. V. Ramanaa, B. L. Jadhavb, *Bioorg. Chem.* **2020**, *96*, 103589.
[7] A. Arafath, F. Adam, F. S. R. Al-Suede, M. R. Razali, M. B. K. Ahamed, A. M. S. A. Majid, M. Z. Hassan, H. Osman, S. Abubakar, *J. Mol. Struct.* **2017**, *1*(149), 216.
[8] M. Imrana, A. Irfan, M. Ibrahim, M. A. Assiri, N. Khalid, S. Ullaha, A. G. Al- Sehemi, *Ind. Crop Prod.* **2020**, *148*, 112285.
[9] F. Beloufa, M. Chikh, *Comput. Methods Programs Biomed.* **2013**, *112*(1), 92.
[10] M. Thirugnanam, P. Kumar, S. V. Srivatsan, C. Nerlesh, *Proc. Eng.* **2012**, *38*, 1709.
[11] K. V. Varma, A. A. Rao, T. S. M. Lakshmi, P. N. Rao, *Comput. Electr. Eng.* **2014**, *40*(5), 1758.
[12] J. Zhu, Q. Xie, K. Zheng, *Inform. Sci.* **2015**, *292*, 1.
[13] M. J. Mphahlele, N. M. Magwaza, S. Gildenhuys, I. B. Setshedi, *Bioorg. Chem.* **2020**, *97*, 103702.
[14] N. H. A. S. Amin, M. Sharma, J. Ahamad, S. R. Mir, *Phytochem. Lett.* **2019**, *32*, 83.
[15] S. Akkoç, B. Tüzün, A. Özalp, Z. Kökbudak, *J. Mol. Struct.* **2021**, *1*(246), 131127.
[16] K. Karrouchi, S. Fettach, E. H. Anouar, B. Tüzün, S. Radi, A. I. Alharthi, H. A. Ghabbour, Y. N. Mabkhot, M. E. A. Faouzi, M.'. Ansar, Y. Garcia, *J. Mol. Struct.* **2021**, *1245*, 131067.
[17] K. M. Kadish, K. M. Smith, R. Guilard, *The Porphyrin Handbook*, first ed. Vol. 11–20, Academic Press, San Diego **2003**.
[18] P. Thordarson, R. J. M. Nolte, K. M. Kadish, K. M. Smith, R. Guilard (Eds), *The Porphyrin Handbook*, Academic Press, San Diego **2003** 281.
[19] L. Liu, X.-F. Zhang, *J. Mol. Struct.* **2022**, *1247*, 131422.
[20] H. Yalazan, K. Tekintaş, V. Serdaroğlu, E. T. Saka, N. Kahriman, H. Kantekin, *Inorg. Chem. Commun.* **2020**, *118*, 107998.
[21] Y. Zhao, K.-Q. Zou, W.-X. Zheng, C.-C. Huang, B.-Y. Zheng, M.-R. Ke, J.-D. Huang, *Dyes and Pigments* **2022**, *199*, 110037.
[22] M. Yahya, Y. Nural, Z. Seferoğlu, *Dyes and Pigments* **2022**, *198*, 109960.
[23] İ. Değirmencioğlu, K. İren, İ. Yalçin, C. Göl, M. Durmuş, *J. Mol. Struct.* **2022**, *1249*, 131599.
[24] H. Yalazan, M. Köç, S. Fandaklı, A. Nas, M. Durmuş, H. Kantekin, *Polyhedron* **2019**, *170*, 576.
[25] L. Kumari, S. A. Mazumder, D. Pandey, M. S. Yar, R. Kumar, R. Mazumder, M. Sarafroz, M. J. Ahsan, V. Kumar, S. Gupta, *Mini-Reviews Org. Chem.* **2019**, *16*, 653.
[26] M. H. A. Soliman, I. A. I. Ali, S. S. A. el-Sakka, O. E. S. A. B. Mohamed, *J. Mol. Struct.* **2022**, *1254*, 132325. https://doi.org/10.1016/j.molstruc.2021.132325
[27] L. K. Salahuddin, A. Mazumder, D. Pandey, M. Shahar Yar, R. Kumar, R. Mazumder, M. Sarafroz, M. Jawed Ahsan, V. Kumar, S. Gupta, *Mini-Reviews in Organic Chemistry* **2009**, *16*, 653.
[28] M. Taha, S. Sultan, S. Imran, F. Rahim, K. Zaman, A. Wadood, A. U. Rehman, N. Uddin, K. M. Khan, *Bioorg. Med. Chem.* **2019**, *27*, 4081.
[29] Ü. Demirbaş, B. Barut, A. Özel, H. Kantekin, *J. Mol. Struct.* **2019**, *1187*, 8.

[30] B. Barut, Ü. Demirbaş, *J. Organomet. Chem.* **2020**, *923*, 121423.
[31] Z. Biyiklioglu, H. Baş, D. Akkaya, B. Barut, *Appl. Organomet. Chem.* **2022**, *36*, e6580. https://doi.org/10.1002/aoc.6580
[32] T. Arslan, *J. Organomet. Chem.* **2021**, *951*, 122021.
[33] E. Güzel, Ü. M. Koçyiğit, P. Taslimi, S. Erkan, O. S. Taskin, *J. Biochem. Mol. Toxicol.* **2021**, *35*, 1. https://doi.org/10.1002/jbt.22765
[34] A. Günsel, A. Yıldırım, P. Taslimi, Y. Erden, T. Taskin-Tok, H. Pişkin, A. T. Bilgiçli, İ. Gülçin, M. N. Yarasir, *Inorg. Chem. Commun.* **2022**, *138*, 109263.
[35] E. Güzel, Ü. M. Koçyiğit, P. Taslimi, İ. Gülçin, S. Erkan, M. Nebioğlu, B. S. Arslan, İ. Şişman, *J. Biomol. Struct. Dyn.* **2022**, *40*, 733.
[36] P. Taslimi, F. Türkan, D. G. Solğun, A. Aras, Y. Erden, H. U. Celebioglu, B. Tuzun, M. S. Ağırtaş, S. Günay, İ. Gülçin, *J. Biomol. Struct. Dyn.* **2022**, *40*, 2991. https://doi.org/10.1080/07391102.2020.1844051
[37] N. Daban, E. B. Orman, L. Meyancı, A. Altındal, M. Özer, A. R. Özkaya, *J. Mol. Struct.* **2022**, *1250*, 131707.
[38] Z. Bıyıklıoğlu, İ. Acar, *Synth. Met.* **2012**, *162*, 1156.
[39] B. S. Jilani, P. Malathesh, C. D. Mruthyunjayachari, K. V. Reddy, *Mater. Chem. Phys.* **2020**, *239*, 121920.
[40] M. Çamur, V. Ahsen, M. Durmuş, *J. Photochem. Photobiol. A Chem.* **2011**, *219*, 217.
[41] J. Chen, Y. Wang, Y. Fang, Z. Jiang, A. Wang, J. Xue, *Biomed. Opt. Express* **2020**, *11*, 3900.
[42] D. Vautherin, D. M. Brink, *Phys. Rev. C* **1972**, *5*, 626.
[43] P. J. Stephens, F. J. Devlin, C. F. Chabalowski, M. J. Frisch, *J. Phys. Chem.* **1994**, *98*, 11623.
[44] K. B. Wiberg, *J. Comput. Chem.* **2004**, *25*, 1342.
[45] A. D. Becke, *J. Chem. Phys.* **1993**, *98*, 5648.
[46] E. G. Hohenstein, S. T. Chill, C. D. Sherrill, *J Chem Theory Comput.* **2008**, *4*, 1996.
[47] D. M. Tanenbaum, Y. Wang, S. P. Williams, P. B. Sigler, *Proc. Natl. Acad. Sci.* **1998**, *95*(11), 5998–6,003.
[48] K. Okamoto, M. Ikemori-Kawada, A. Jestel, K. von König, Y. Funahashi, T. Matsushima, A. Tsuruoka, A. Inoue, J. Matsui, *ACS Med. Chem. Lett.* **2015**, *6*(1), 89.
[49] A. A. Marusiak, N. L. Stephenson, H. Baik, E. W. Trotter, Y. Li, K. Blyth, S. Mason, P. Chapman, L. A. Puto, J. A. Read, C. Brassington, H. K. Pollard, C. Phillips, I. Green, R. Overman, M. Collier, E. Testoni, C. J. Miller, T. Hunter, O. J. Sansom, J. Brognard, *Cancer Res.* **2016**, *76*(3), 724.
[50] J. Anantharajan, H. Zhou, L. Zhang, T. Hotz, M. Y. Vincent, M. A. Blevins, A. E. Jansson, J. W. L. Kuan, E. Y. Ng, Y. K. Yeo, N. Baburajendran, G. Lin, A. W. Hung, J. Joy, S. Patnaik, J. Marugan, P. Rudra, D. Ghosh, J. Hill, T. H. Keller, R. Zhao, H. L. Ford, C. B. Kang, *Mol. Cancer Ther.* **2019**, *18*(9), 1484.
[51] S. Salentin, S. Schreiber, V. J. Haupt, M. F. Adasme, M. Schroeder, *Nucleic Acids Res.* **2015**, *43*(W1), W443.
[52] M. Taha, F. Rahim, N. Uddin, I. Ullah Khan, N. Iqbal, E. H. Anouar, M. Salahuddin, R. K. Farooq, M. Gollapalli, K. M. Khan, A. Zafari, *Int. J. Biol. Macromol.* **2021**, *188*, 1025.
[53] H. Pashaei, A. Rouhani, M. Nejabat, F. Hadizadeha, S. Mirzaei, H. Nadri, M. F. Maleki, R. Ghodsi, *J. Mol. Struct.* **2021**, *1244*, 130919.
[54] E. Kırbaç, A. Erdoğmuş, *J. Mol. Struct.* **2020**, *1202*, 127392.
[55] a) B. S. Ajilore, A. A. Alli, T. O. Oluwadairo, *Pharmacol. Res. Perspect.* **2018**, *6*, e00401; b) F. Ibrahim, Y. C. Guillaume, M. Thomassin, C. André, *Talanta* **2009**, *79*, 804.
[56] V. G. Klochkov, E. N. Bezsonova, M. Dubar, D. D. Melekhina, V. V. Temnov, E. V. Zaryanova, N. A. Lozinskaya, D. A. Babkov, A. A. Spasov, *Bioorg. Med. Chem. Lett.* **2022**, *55*, 128449.
[57] S. Wang, Y. Li, D. Huang, S. Chen, Y. Xia, S. Zhu, *Food Chem.* **2022**, *372*, 131334.
[58] A. Günsel, P. Taslimi, G. Yaşa Atmaca, A. T. Bilgiçli, H. Pişkin, Y. Ceylan, A. Erdoğmuş, N. Yarasir, İ. Gülçin, *J. Mol. Struct.* **2021**, *1237*, 130402.
[59] A. Şenocak, N. A. Taş, P. Taslimi, B. Tüzün, A. Aydin, A. Karadağ, *J. Biochem. Mol. Toxicol.* **2021**, *36*, e22969.
[60] A. L. F. Sarria, A. F. L. Vilela, B. M. Frugeri, J. B. Fernandes, R. M. Carlos, M. F. da Silva, Q. B. Cass, C. L. Cardoso, *J. Inorg. Biochem.* **2016**, *164*, 141.
[61] D. Avcı, S. Altürk, F. Sönmez, Ö. Tamer, A. Başoğlu, Y. Atalay, B. Zengin Kurt, N. Dege, *J. Mol. Struct.* **2019**, *1197*, 645.
[62] W. Ishaniya, M. Ganeshpandian, *Materials Today: Proceedings* **2022**, *50*, 358. https://doi.org/10.1016/j.matpr.2021.10.013
[63] S. Jahani, Z. Aramesh-Boroujeni, M. Noroozifar, *J. Trace Elem. Med. Biol.* **2021**, *68*, 126821.
[64] B. Barut, Ü. Demirbaş, A. Özel, H. Kantekin, *Int. J. Biol. Macromol.* **2017**, *105*, 499.
[65] B. Barut, Ü. Demirbaş, *J. Organomet. Chem.* **2020**, *923*, 121423.
[66] S. B. Kedare, R. P. Singh, *J. Food Sci. Technol.* **2011**, *48*(4), 412.
[67] M. P. de Torre, R. Y. Cavero, M. I. Calvo, J. L. Vizmanos, *Antioxidants* **2019**, *8*, 142. https://doi.org/10.3390/antiox8050142
[68] A. T. Bilgiçli, H. Genc Bilgicli, C. Hepokur, B. Tüzün, A. Günsel, M. Zengin, M. M. Yarasir, *Appl. Organomet. Chem.* **2021**, *35*, e6242.
[69] F. Türkan, P. Taslimi, B. Cabir, M. S. Ağırtaş, Y. Erden, H. U. Celebioglu, B. Tuzun, E. Bursal, I. Gulcin, *Polycyclic Aromatic Compounds* **2021**, 1.
[70] M. Erdoğan, P. Taslimi, B. Tuzun, *Arch. Pharm.* **2021**, *354*(6), 2000409.
[71] A. Poustforoosh, S. Faramarz, M. H. Nematollahi, H. Hashemipour, B. Tüzün, A. Pardakhty, M. Mehrabani, *J. Cell. Biochem.* **2021**, *123*, 390.
[72] M. Gömeç, F. Yulak, H. Gezegen, M. Özkaraca, K. Sayin, H. Ataseven, *J. Mol. Struct.* **2022**, *1254*, 132318.
[73] A. T. Bilgiçli, T. Kandemir, B. Tüzün, R. Arıduru, A. Günsel, Ç. Abak, M. N. Yarasir, G. Arabaci, *Appl. Organomet. Chem.* **2021**, *35*(10), e6353.

SUPPORTING INFORMATION

Additional supporting information may be found in the online version of the article at the publisher's website.

How to cite this article: H. Yalazan, B. Tüzün, D. Akkaya, B. Barut, H. Kantekin, S. Yıldırmış, *Appl Organomet Chem* **2022**, e6696. https://doi.org/10.1002/aoc.6696